Magnetoelectric Dipole Antenna Arrays

Shulabh Gupta, *Member, IEEE*, Li Jun Jiang, *Senior Member, IEEE*, and Christophe Caloz, *Fellow, IEEE*

***Abstract*—A planar magnetoelectric (ME) dipole antenna array is proposed and demonstrated by both full-wave analysis and experiments. The proposed structure leverages the operation of composite right/left-handed transmission lines under balanced conditions to form high-gain magnetic radiators, combined with radial conventional electric radiators, where the overall structure is excited by a single differential feed. The traveling-wave-type nature of the proposed ME-dipole antenna enables the formation of directive arrays with high-gain characteristics and scanning capability. Peak gains of 10.84 dB and 5.73 dB are demonstrated for the electric dipole and magnetic-dipole radiation components, respectively.**

***Index Terms*—Antenna array, composite right/left-handed (CRLH) transmission line, frequency beamscanning, leaky-wave antenna, magnetoelectric (ME) dipole, traveling-wave structure.**

I. Introduction

THE CONCEPT of collocated magnetic and electric dipole radiators (M- and E-dipoles) has recently attracted considerable attention due to the increased demand for multifunctionality and switchable characteristics in modern communication systems [1]. Applications include anticollisions systems for vehicular transport [2], multiple-input multiple-output (MIMO) systems for high-speed communication [3], and enhanced polarization diversity MIMO systems [4] for instance. While conventional phase-array antennas have been sporadically used in such applications, [5]–[7], a clever combination of the two fundamental types of radiators, namely, magnetic and electric dipoles, into a magnetoelectric (ME) antenna, may offer enhanced performance functionalities.

The concept of ME antennas was introduced in [8], where identical E- and H-plane radiation patterns are obtained by exciting simultaneously an electric dipole and a magnetic dipole. This concept was further explored in slot configurations in [9] and analyzed for an array in [10] and recently for ultrawideband (UWB) applications in [11] and [12] for resonant-type configurations. These ME antennas are nonplanar and are difficult to fabricate. A planar ME monopole configuration based on composite right/left-handed (CRLH) transmission lines was proposed in [13] and [14], but it requires a dual-feeding mechanism to excite the E- and M-radiators separately. Moreover, being a resonant type (as opposed to a traveling-wave type), it cannot be used to form a single-feed array.

In this paper, an ME-dipole antenna structure is proposed in a planar configuration based on CRLH transmission lines, where the electric and magnetic radiators are excited simultaneously using a single differential feed. While E- and M-radiators are conventionally used in a superposed configuration where the two radiators enhance each other to form a single radiating element [11], [12], the proposed structure acts as two distinct antennas in one structure with their individual radiation characteristics. Furthermore, compared to conventional resonant-type ME antennas, the proposed antenna is travelling wave in nature, which makes it suitable for forming simple high-gain ME-dipole antenna arrays with dual-polarized radiation characteristics [15], [16]. Finally, due to the CRLH leaky-wave property of the structures, the proposed structure offers frequency beamscanning of E- and M-dipoles.

This paper is organized as follows. Section II introduces the concept of ME-dipole antennas based on CRLH structures. Using a typical implementation of a CRLH-based structure, the radiation characteristics of the proposed ME-dipole antenna are described in details and modelled using an array factor theory to provide further insight into the structure. Section III presents the experimental prototypes of the ME-dipole antenna array and its beamswitching characteristics. Finally, conclusions are provided in Section IV.

II. ME Dipole Antenna Array

A. Structure and Principle

Consider the structure of Fig. 1(a) consisting of a magnetic loop dipole and an electric-wire dipole placed within it along the radial direction, where each of the two dipoles has its own and independent differential excitation. When the two dipoles are excited simultaneously, combined magnetic and dipole radiation is achieved in the far field of the structure. Such a combined radiator is referred to as an ME-dipole antenna. Although being straightforward, this configuration is unpractical because it requires two separate and intertwined feeds. However, this antenna can be replaced by the merged structure shown in Fig. 1(b) with $Z_0 = 0$ (direct loop connection), where the ring is differentially excited from two antipodal points, where part of the loop current is used to drive the electric dipole at the center of the ring. This structure is more practical since it uses a *single differential excitation*. Moreover, if a second differential port, of impedance $Z_0 \neq 0$, is placed at the other side of the loop, the

Manuscript received August 23, 2013; revised January 12, 2014 and April 16, 2014; accepted April 22, 2014. Date of publication April 30, 2014; date of current version July 02, 2014. This work was supported in part by HK ITP/026/11LP, in part by HK GRF 711511, in part by HK GRF 713011, in part by HK GRF 712612, and in part by NSFC 61271158.

S. Gupta and L. J. Jiang are with the Electrical and Electronic Engineering Department, University of Hong Kong, Hong Kong, China (e-mail: shulabh@hku.hk).

C. Caloz is with the Department of Electrical Engineering, PolyGrames Research Center, École Polytechnique de Montréal, Montréal, QC H3T 1J4 Canada.

Color versions of one or more of the figures in this paper are available online at http://ieeexplore.ieee.org.

Digital Object Identifier 10.1109/TAP.2014.2320531

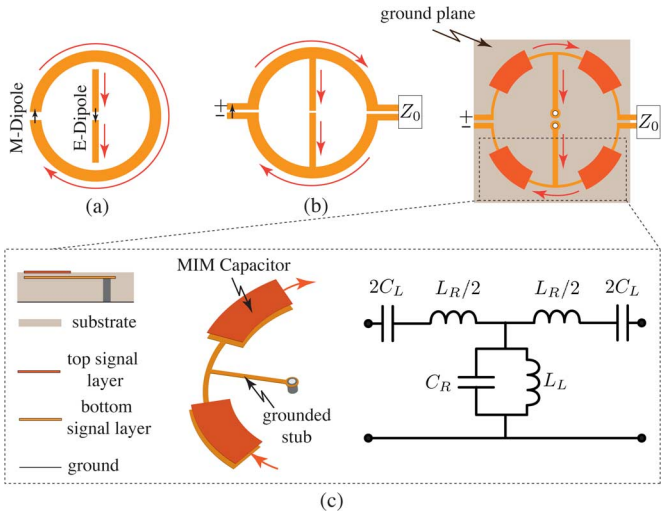

Fig. 1. Proposed planar magnetoelectric (ME) antenna. (a) Colocated E- and M-dipoles with separate feeds. (b) Two-port traveling-wave configuration consisting of merged colocated E- and M-dipoles with a common differential feed. (c) Composite right/left-handed (CRLH) implementation of the ME-dipole operating in the balanced condition and radiating into the half-space above the ground plane.

structure transforms from a *resonant-type* to a *traveling-wave*-type antenna.

It is well known that the gain of a magnetic loop dipole is small but it can be theoretically improved by increasing the size of the loop while maintaining the current along the loop constant [17]. This can be practically achieved by using a composite right/left-handed (CRLH) transmission line structure operating in the balanced condition [14], [18]–[20]. A CRLH transmission line is a periodic structure whose unit-cell consists of a series capacitance C_L and a shunt inductance L_L in addition to a series inductance L_R and shunt capacitance C_R, as shown in the circuit model of Fig. 1(c) [21]. A common implementation of a CRLH transmission line is the metal-insulator-metal (MIM) implementation also illustrated in the figure. The parallel-plate MIM capacitor provides C_L and the shunt stub connected to ground using a conducting via, provides L_L. The other elements L_R and C_R are modelled using a series transmission-line section and a shunt stub, respectively. This artificial transmission line acts as a left-handed (LH) transmission line at low frequencies and a right-handed (RH) transmission line at high frequencies. It has been extensively applied in realizing both guided-wave and radiative components, including phase shifters [22], [23]; tight couplers; as well as leaky-wave and phase-array antennas [14], [7], among many other applications. A CRLH transmission line is characterized by the following dispersion relation [14]:

$$\beta(\omega) = \frac{1}{p}\cos^{-1}\left(1 - \frac{\kappa}{2}\right) \tag{1a}$$

where

$$\kappa = \left(\frac{\omega}{\omega_R}\right)^2 + \left(\frac{\omega_L}{\omega}\right)^2 - \kappa\omega_L^2 \tag{1b}$$

with $\kappa = L_L C_R + L_R C_L$, $\omega_R = 1/\sqrt{L_R C_R}$, and $\omega_L = 1/\sqrt{L_L C_L}$, which corresponds to the dispersion relation of the CRLH radiation space harmonic, the harmonic $n = 0$, featuring $\beta = 0$ at the transition frequency between the LH and RH bands [14], [21]. Depending on the relative values of the LH and RH contributions, this transmission line can be unbalanced or balanced, that is, exhibiting or not exhibiting a gap between the two bands. The balanced condition requires that the individual elements be designed such that $L_L C_R = L_R C_L$, which is also the condition for broadband matching [14]. Under the balanced condition, the CRLH propagation constant simplifies to

$$\beta(\omega) = \left(\frac{\omega}{\omega_R} - \frac{\omega_L}{\omega}\right). \tag{2}$$

The frequency, where the dispersion curve passes from the LH band to the RH band, $\beta = 2\pi/\lambda_g = 0$, is referred to as the transition frequency. At this frequency, the structure operates under a balanced condition and supports a traveling wave with $v_g = d\omega/d\beta \neq 0$. This $\beta = 0$ regime has some similarity with the cutoff regime in a waveguide, but with the essential difference that it supports a traveling wave exactly at $\beta = 0$. Consequently, the phase of the fields on the structure is macroscopically uniform along the CRLH transmission-line structure, irrespective of its length. Moreover, a CRLH transmission line can also operate in a radiative leaky-wave mode when open to free space, since the CRLH dispersion curve penetrates into the fast-wave region, where the phase velocity $v_p(\omega) = \omega/\beta(\omega)$ is larger than the speed of light [14], [24], [25]. The resulting leaky-wave antenna (LWA) radiates from backfire to end fire, including broadside, since the frequency is scanned from the backward to forward regions [26], [27]. It is to be noted that rigorous conditions exist to achieve a seamless transition from the LH band to the right-hand band, to ensure that the resulting CRLH structure is balanced, without any gain drop at the broadside while scanning from the backward to forward region [28].

These unique properties can be leveraged to transform the ME-dipole structure of Fig. 1(b) to that shown in Fig. 2(a), where the series radiation component of the CRLH transmission line forms the current loop, that is, the M-dipole and the shunt radiation component forms the E-dipole. Then, owing to the balanced condition of the CRLH transmission line at the transition frequency, the size of the ring can be made arbitrarily large without altering the current phase or wave-propagation direction. Consequently, compared to the conventional resonant loop antennas, the operation frequency of the CRLH loop does not depend on the size of the ring, but on the transition frequency depending on the unit-cell design of the CRLH structure. The M-dipole gain can be progressively increased by increasing the size of the current loop, as shown in Fig. 2(a), with a larger number of unit cells while maintaining the balanced condition at the design frequency. The circular array of shunt radiation components contributes to the E-dipole contribution where all radial electric dipoles have cancelling parts in the horizontal direction, to generate a global vertical dipole, as shown in Fig. 2(a). It is to be noted that compared to the ME-dipole of Fig. 1(b), the CRLH-based implementation typically requires ground-plane restricting radiation to half-space in contrast to the bidirectional radiation of conventional dipole antennas.

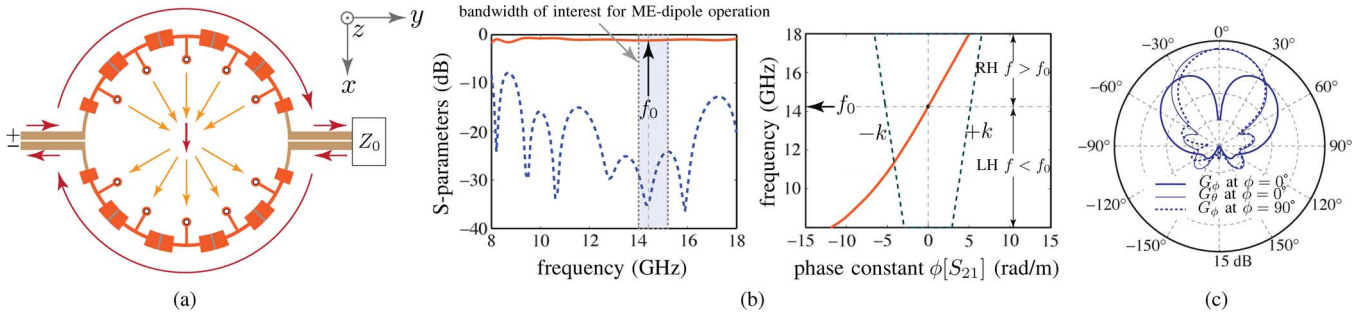

Fig. 2. Proposed ME-dipole antenna based on CRLH transmission lines operating in the balanced condition, where the size of the ring, in principle, can be made arbitrarily large to enhance the gain. (a) Structure layout. (b) S-parameters for $N = 5$ unit cells and their corresponding transmission phase $\phi[S_{21}]$ with $Z_0 = 100\ \Omega$, and c) typical radiation patterns at broadside, computed using FEM-HFSS. The physical parameters used are the same as in Fig. 3. The G_θ component at $\phi = 90°$ is negligible.

Fig. 2(b) shows typical S-parameters and the dispersion diagram of such a CRLH structure. Good matching is clearly apparent across a wide frequency band, including the transition frequency f_0. A seamless transition from the LH to the RH band is clearly observed in the dispersion diagram in Fig. 2(b). The part of the dispersion curve crossing the triangular fast-wave region corresponds to leaky-wave radiation. In particular, the transition frequency f_0 points to the broadside direction [21]. While the CRLH structure is wideband as evident from the S-parameters of Fig. 2(b), the usable bandwidth for ME-dipole radiation is restricted around the narrow frequency band around the transition frequency f_0 due to the rapid degradation of the uniform current distribution when operating away from f_0.

B. Features and Benefits

Compared to conventional ME-dipole antennas, the proposed antenna offers the advantage of combining *all* of the following benefits:

1) It is easy to fabricate, due to its *planar configuration*, and is compatible with MMIC technology.
2) It has a simple configuration requiring only a *single differential feed* to excite the E and M dipoles.
3) As opposed to resonant-type ME-dipole antennas, the proposed structure is of *traveling-wave type* and, therefore, can be extended to a single-feed array configuration for high-gain and scanning performance.
4) The proposed antenna has a *radiation characteristic* that is capable of frequency scanning in two orthogonal planes with orthogonally polarized fields components. Fixed-frequency beamscanning can naturally be achieved using voltage-controlled varactors integrated in the antenna [14].
5) Due to its intrinsic differential nature, the proposed antenna is compatible with *high-density circuits* [29] and, in particular, can be naturally integrated with differential amplifiers for *beamshaping* and *beamforming* applications [30]–[32].

C. Antenna Array Configuration

As mentioned in the previous sections, placing a second differential port on the current loop of Fig. 1(b) and (c) converts the ME-dipole antenna into a *traveling-wave-type antenna*. This enables the realization of an ME-dipole antenna array, as shown in Fig. 3(a), consisting of $N = 6$ rings,[1], offering the possibilities for enhanced gain and directivity performance. This structure may be seen as a phase-array antenna, where each circular unit consisting of electric and magnetic dipole antennas, radiates a leaky wave following the CRLH dispersion characteristic [33].

The typical radiation patterns of such an array are shown in Fig. 3(b) and (c) for the transition frequency $f_0 = 14.25$ GHz and frequencies f_{LH} and f_{RH} in the LH band and RH band of the CRLH transmission line, respectively. At this frequency, the ME-dipole array is about $4.6\lambda_0$ in the y-direction, and the corresponding CRLH structure is $6.5\lambda_0$ following the circumference of the rings. Fig. 3(b) shows the components E_x and E_y for each frequency, and Fig. 3(c) shows the corresponding 2-D patterns in three principal cuts. Observations can be made from these patterns as follows.

1) The E_y field component corresponds to the M-dipole contribution only and exhibits a typical radiation pattern of a loop antenna over a ground plane with a null at $\theta = 0°$.
2) The E_x field component corresponds primarily to the E-dipole contribution and exhibits a minimum at $\theta = \pm 90°$.
3) Full-space scanning from the backward to forward regions, including broadside, is achieved for the E- and M-dipoles, as typical in CRLH leaky-wave antennas.
4) While the E-dipole components E_ϕ scan in the $\phi = 90°$ plane, the M-dipole scans in the $\theta = 90°$ plane with E_ϕ polarization.
5) While the E-dipole pattern has a single beam in $+z$-space, the M-dipole pattern exhibits two beams, one in each positive $x - z$ plane quadrants.
6) There is only one dominant field component E_ϕ in the $x-y$ and $y - z$ planes, along with zero cross-polarization E_θ.

The S-parameters and gain performance of this array design are shown in Fig. 3(d). Good matching is obtained around the transition frequency f_0, with a seamless transition from the LH to the RH frequency band, as is clearly evident from the corresponding continuous transmission phase across f_0, also shown in Fig. 3(d). Both E- and M-dipoles exhibit a high peak gain greater than 10 dB within the bandwidth of interest around the transition frequency. For example, a substantial

[1]The choice of $N = 6$ rings is to ensure that the structure can be fabricated using the multilayer process at our facility, which is restricted to 12.7×6.4 cm of area.

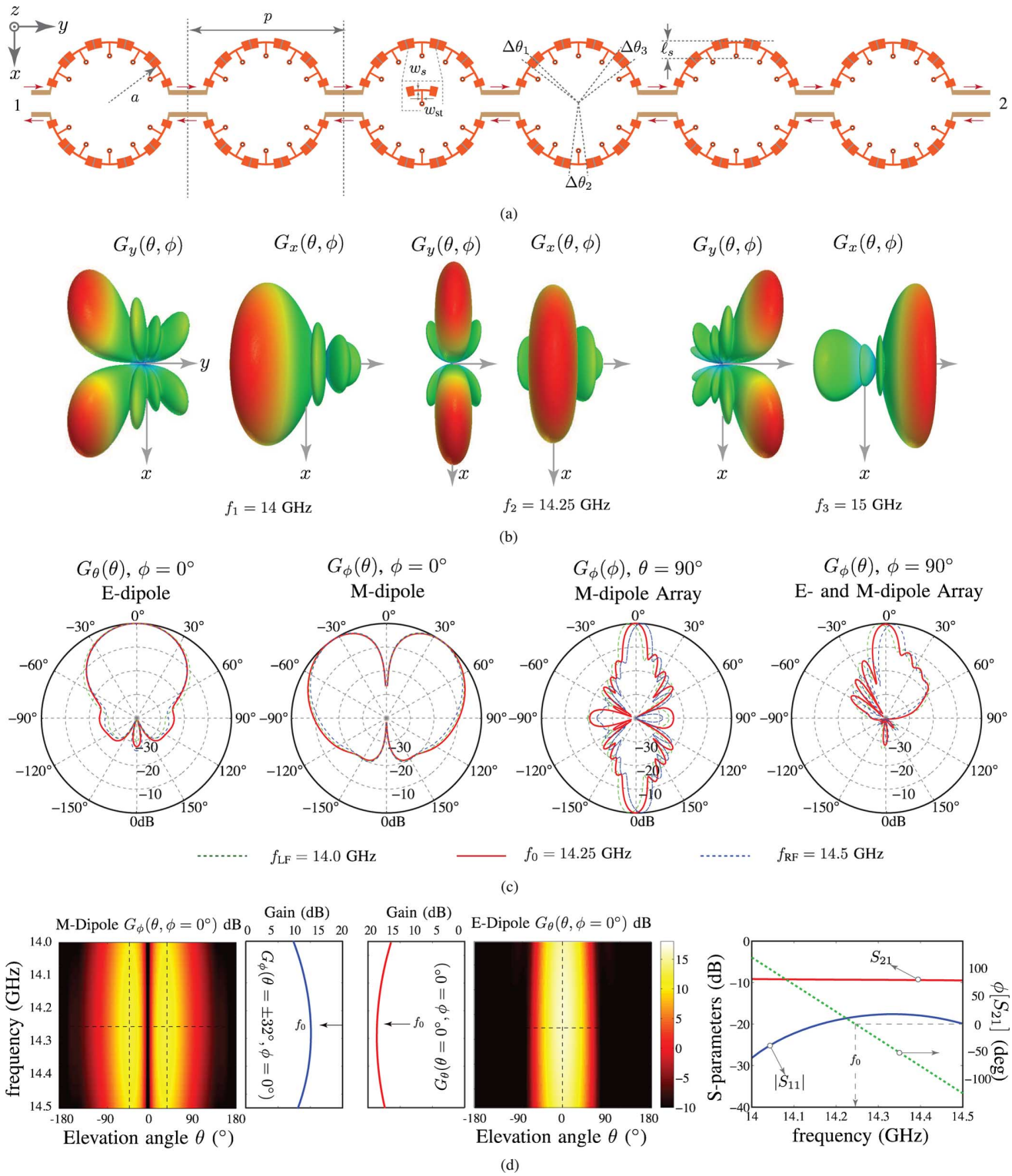

Fig. 3. Proposed ME-dipole antenna array. (a) Structure layout with each CRLH unit cell implemented in metal-insulator-metal (MIM) technology. (b) Typical 3-D normalized radiation patterns at the transition frequency $f_0 = 14.25$ GHz of the CRLH structure and the frequencies $f_{\rm LF} = 14.0$ GHz and $f_{\rm RF} = 15.0$ GHz in the left- and right-hand bands, respectively, computed using FEM-HFSS. (c) Normalized radiation patterns in three coordinate planes. (d) Typical realized gain pattern patterns including dissipation losses and antenna mismatch showing the M- and E-dipole gains along with the two-port S-parameters. The structure consists of two substrates (Taconic RF-30 $\varepsilon_r = 3$) with a height of 0.508 mm and 0.127 mm, respectively. The structural parameters are $p = 16$ mm, $a = 7$ mm, $w_s = 0.254$ mm, $w_{\rm st} = 0.254$ mm, $\ell_s = 2$ mm, $\Delta\theta_1 = 6°$, and $\Delta\theta_2 = \Delta\theta_3 = 15°$. The via radius is 0.254 mm and the ground-plane width is $6a$.

increase in the gain at broadside is achieved compared to that of a single-ring structure, as seen from Fig. 3(c). The gain map of the M-dipole shows that the maximum gain at individual frequencies occurs at about $\theta = \pm 32°$ due to the presence of the finite-size ground plane, instead of $\theta = \pm 90°$. Across the frequency range, the transition frequency exhibits the highest gain, for E- and M-dipole radiation components, with a smooth drop in gain on either side of it. This is expected as the uniform

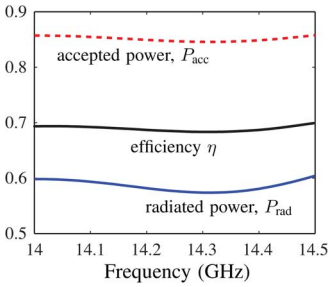

f (GHz)	14.0	14.25	14.5
P_{acc}	0.86	0.85	0.85
P_{rad}	0.59	0.58	0.60
η (%)	69.3	68.8	69.5
η_p^M (%)	25.7	40.0	27.1
η_p^E (%)	84.2	100.0	66.5

Radiation efficiency $\eta = \frac{P_{rad}}{P_{acc}}$

aperture efficiency $\eta_p = \frac{G\lambda^2}{4\pi A_p}$

Fig. 4. Various radiation performance parameters of the ME-dipole array of Fig. 3, computed using FEM-HFSS.

current distribution is only achieved at f_0. At other frequencies, the current distribution deviates from the uniform distribution; therefore, the gain subsequently drops due to spatial dispersion. This sensitivity of the current distribution across the ring structure makes the proposed ME-dipole antenna *narrowband*. Fig. 4 summarizes the performance of the antenna of Fig. 3. A fairly constant antenna efficiency of about 69% is seen across the bandwidth of interest.

Fig. 5(a) shows full-wave computed E-field plots in the near-field region of the antenna, in the two orthogonal planes $z =$ 10 mm and $x = 0$ at the transition frequency f_0. As expected, a uniform field profile is observed across the structure, confirming the balanced operation of the CRLH structure. The decrease in the field amplitude along the y-axis is due to the leaky-wave radiation loss and the power dissipation in the conductor and the dielectric. The corresponding total E-field distribution along the antenna $|E(y)|$ at two different locations above the antenna shows that the plane waves start to form at about $z = 10$ mm, which corresponds to roughly a half-wavelength distance from the antenna, that is, $\lambda_0/2$ at f_0. Fig. 5(b) shows the magnitude and phase of the dominant E_x component of the electric field, corresponding to the electric dipole radiation, with a near-uniform phase profile in accordance with the balanced operation of the CRLH structure.

D. Comparison With an Array of Ideal Dipole Radiators

As mentioned before, the proposed CRLH ME-dipole antenna, based on the CRLH structure, may be seen as an array of uniform current loops of uniform current, collocated with short electric dipoles, as shown in Fig. 2. To confirm the validity of this equivalence, an array of ideal current loops and dipoles is considered, as shown in Fig. 6(a). This array consists of $N = 6$ differentially excited rings of radius r_0 and circumference C, along with collocated short electric dipoles of length ℓ, with their own differential excitations, on top of a grounded substrate to model a unidirectional radiation pattern similar to the proposed ME-dipole structure. The separation p between the radiating units is taken to be the same as that used in Fig. 3 for fair comparison. Furthermore, all of the radiating elements are simultaneously excited to emulate the broadside operation of the array. Consequently, all of the forthcoming comparisons are made at the transition frequency, with $\beta = 0$, of the ME-dipole array, that is, $f_0 = 14.25$ GHz.

Fig. 6(b) shows the comparison of the simulated radiation patterns of the ideal structure with the proposed ME-dipole array, under two different conditions:

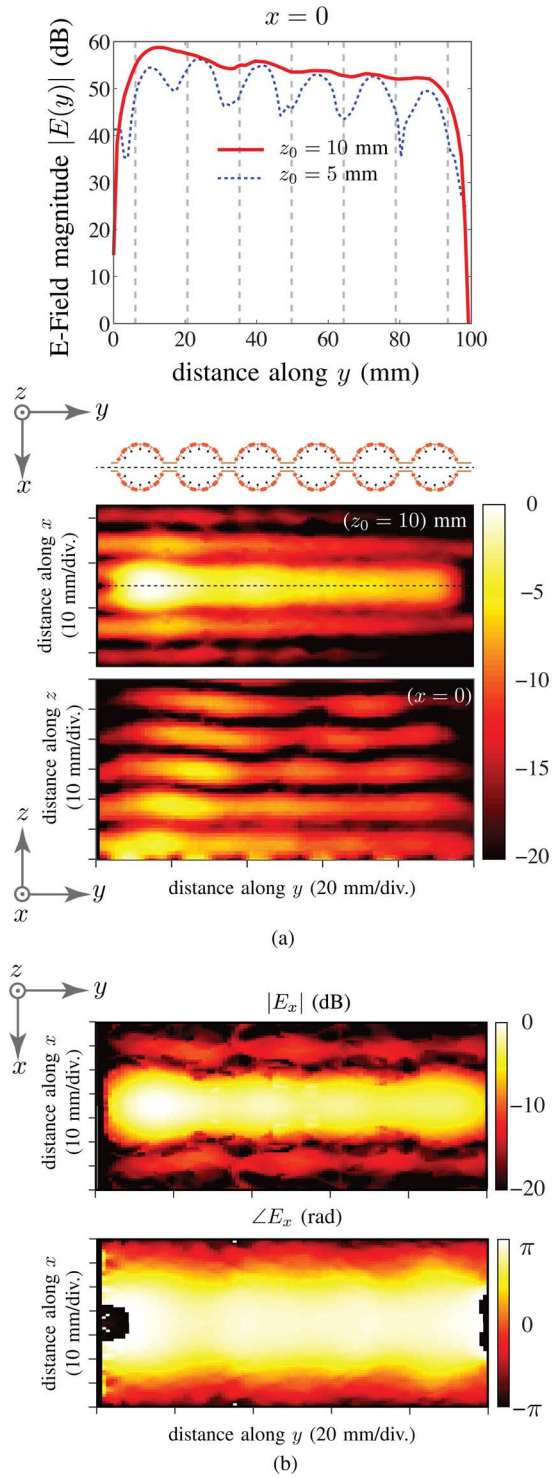

Fig. 5. Full-wave (FEM-HFSS) computed near fields just above the ME-dipole array of Fig. 3(a) at the transition frequency $f_0 = 14.25$ GHz. (a) Total E-fields at $x = 0$ and $z_0 = 10$-mm planes, and b) magnitude and phase of the dominant E_x component of the electric field at $z_0 = 10$ mm. All E-field magnitude profiles represent instantaneous phases.

1) Case I $C \approx 0.67\lambda_0$: In this case, the conventional loop antennas have a close to uniform current distribution [17]. The following observations can be made:
   - A broadside null is achieved in the magnetic-loop component (i.e., G_ϕ in $\phi = 0°$) of both ideal and CRLH ME-dipole arrays. While the ideal loops are electrically

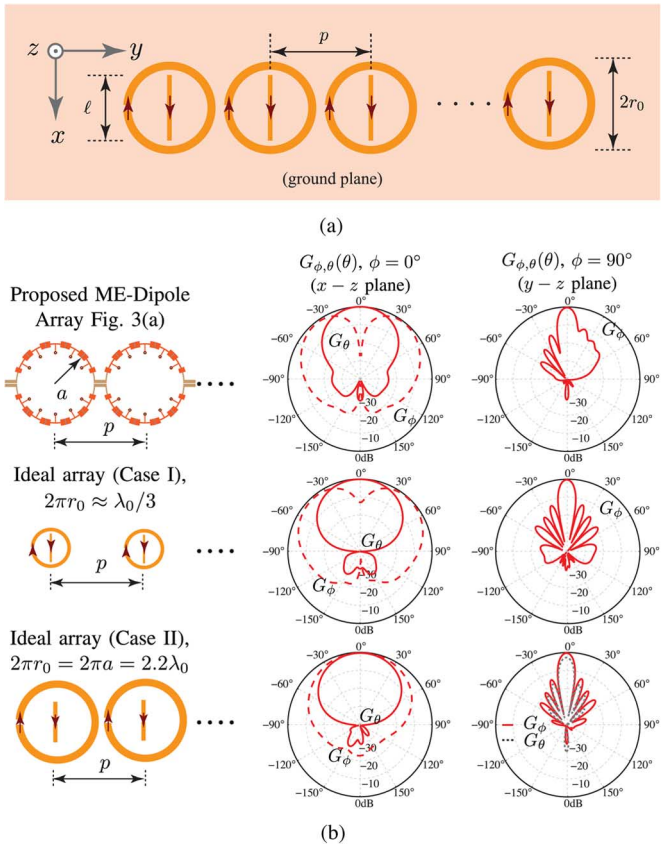

Fig. 6. Radiation patterns comparisons between the proposed and ideal ME-dipole array. (a) An ideal array consisting of colocated current loops and electric dipoles, with their own signal inputs. (b) Full-wave (FEM-HFSS) radiation patterns of the proposed ME-dipole array of Fig. 3 compared with an ideal array formed using small current loops $r_0 \ll \lambda_0$, and a current loop of identical size $r_0 = a$.

small, the CRLH array has a much larger loop circumference ($C \approx 2.2\lambda_0$). This further confirms that the ME-dipole array loop has a uniform current distribution, although it has an electrically large size.

- There is no G_θ component in the $y-z$ plane in both cases, since the electric dipole is orthogonally polarized in both cases.
- A typical electric dipole response is seen in the $x-y$ plane in both cases, with a maximum at broadside. In addition, a directive beam is formed in the $y-z$ plane due to the presence of a copolarized electric-dipole array. This confirms the presence of an equivalent electric dipole located at the center of the ring.

2) Case II $C \approx 2.1$: In this case, the loop is electrically large with a nonuniform-field distribution. Two observations can be made as follows.
   1) A broadside maximum is observed in the magnetic-loop component (i.e., G_ϕ in $\phi = 0°$) of the ideal array, as opposed to the null in the case of the CRLH ME-dipole array.
   2) There is a strong cross-polarization component G_θ in the $y-z$ plane which does not exist in the proposed CRLH array.

They demonstrate that a very different radiation pattern is obtained compared to that of the proposed structure or the ideal structure consisting of electrically small dipoles.

It is to be noted that the grounded array structure considered here is only used for qualitative comparisons of the radiation patterns, to validate its link with the CRLH ME-dipole array. These ideal arrays otherwise, are inefficient radiators primarily due to the presence of a ground plane in the close proximity of the radiating loops and dipoles, which nullifies the far-field radiation due to equal and opposite radiating current images. Consequently, they have negligible gain and very low radiation efficiencies [17]. The proposed CRLH ME-dipole array, based on leaky-wave radiation, may be seen as a practical way to achieve such radiation pattern characteristics with high gain performance, using a single differential feed.

III. Measurement Results

To experimentally demonstrate the ME-dipole antenna array, an MIM 6-ring array similar to that of Fig. 3(a) was fabricated, as shown in Fig. 7(a). The differential excitation of the ME-dipole array is achieved using a four-port rat-race coupler designed at the center frequency f_0, with isolated port terminated with a 50-Ω load. The second port of the antenna array is terminated by a matched 100-Ω load. It may thus be seen as a truncated structure where the power left at the end of the structure is absorbed by the load. The prototype consists of two Taconic RF-30 substrates $\varepsilon_r = 3.0$, which are 0.508 and 0.127 mm thick, respectively, as shown in the inset of Fig. 7(a). A prepreg layer with $\varepsilon_r = 2.42$ and $\tan\delta = 0.02$ from Taconic is used to connect the two substrates together to form the multilayer configuration. The actual thickness of the prepreg layer was not known at the time of the fabrication and, consequently, the suggested thickness of 114 μm from the Taconic datasheet is assumed in modeling this structure in FEM-HFSS.

Fig. 8 shows the measured S-parameters of the fabricated prototype at the input of the rat-race coupler. Matching with $|S_{11}| < -10$ dB is achieved across the bandwidth of interest. The matching at the input of the antenna is also shown, where a differential probe is directly used at the two input terminals of the antenna array, as shown in the photograph of Fig. 8 to measure the input differential return loss S_{11}^{diff}.

The antenna was next measured in an anechoic chamber, and the measured radiation patterns are shown in Fig. 7(b), along two principal cuts. The M-dipole response is clearly evident in the $x-z$ plane with a null at broadside, that is, $\theta = 0°$, coinciding with the maximum radiation of the E-dipole. Typical beamscanning characteristics of the CRLH structure are seen in the $y-z$ plane with the beamscanning from backward ($\theta = -4°$) to forward region ($\theta = +4°$), including broadside radiation ($\theta = 0°$). This broadside radiation corresponds to $f_0 = 14.5$ GHz. The corresponding 2-D radiation patterns are shown in Fig. 7(c) for three selected frequencies $f_{\text{LF}} = 14.25$ GHz in the LH range, transition frequency $f_0 = 14.5$ GHz, and $f_{\text{RH}} = 14.75$ GHz in the RH range of the CRLH structure. Good agreement is obtained between measurements and simulations in all cases. The measured gain values corresponding to the E- and M-dipoles are shown in Fig. 7(d), computed in the $x-z$ plane. The broadside gain of 10.84 dB is achieved for the E-dipole component, compared to the simulated gain of 12.74 dB. Similarly, the M-dipole gains are 10.06 dB and 5.73 dB, corresponding to the two beams in $(-x-z)$ and $(+x-z)$ quadrants,

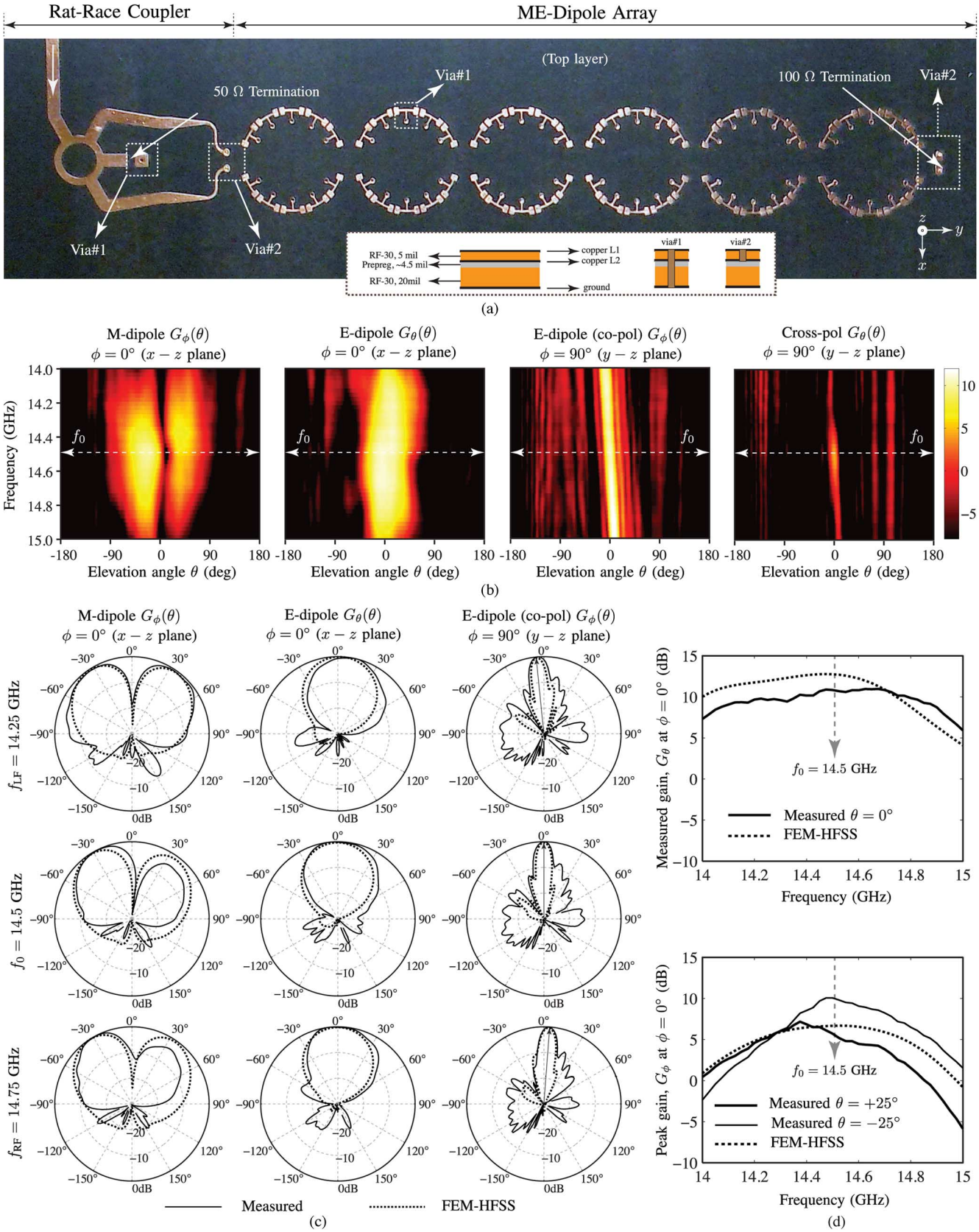

Fig. 7. Fabricated CRLH TL-based ME-dipole array structure and measured radiation patterns compared with FEM-HFSS. (a) Photograph of the antenna structure showing the layout patterns of the top metal layer, along with the layer and via definitions in the inset. (b) Measured radiation patterns of two orthogonal polarizations in $x-z$ and $y-z$ planes. (c) 2-D Radiation patterns of three frequencies corresponding to $f_{\rm LF} = 14.25$ GHz in the LH range, transition frequency $f_0 = 14.5$ GHz, and $f_{\rm RH} = 14.75$ GHz in the RH range of the CRLH structure. (d) Measured peak-gain corresponding to E- and M-dipole components of the ME-dipole array. The structure consists of two substrates of heights, 0.508 mm and 0.127 mm, respectively. The structural parameters are $p = 16$ mm, $a = 7$ mm, $w_s = 0.254$ mm, $w_{\rm st} = 0.254$ mm, $\ell_s = 1.5$ mm, $\Delta\theta_1 = 6.25°$, $\Delta\theta_2 = 16°$, and $\Delta\theta_3 = 14°$. The via radius = 0.254 mm.

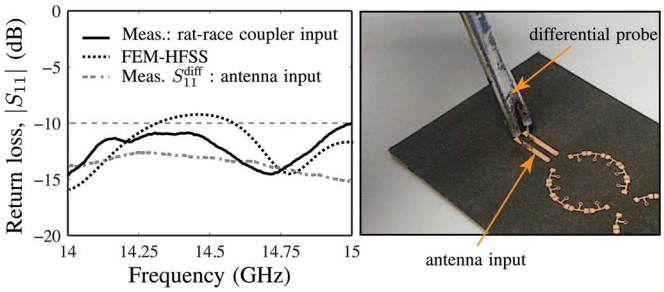

Fig. 8. Measured S-parameters of the ME-dipole array of Fig. 7(a) at the input of the rat-race coupler and the antenna array.

respectively, compared to the simulated gain of 7.2 dB (two beams symmetrical in HFSS). This asymmetry can be attributed to the presence of the rat-race coupler and the SMA connector used in the measurement chamber. This can be easily corrected by choosing a connector suitable for high-frequency measurements and appropriately shielding it. The difference between the measurement and the simulated gains could be attributed to the uncertainty regarding the exact material and structural properties of the prepreg layer used along with high sensitivity to fabrication tolerances at these frequencies.

It is to be noted that the measured transition frequency is shifted by 0.25 GHz toward high frequencies, compared to the design frequency of 14.25 GHz (see Fig. 3). This shift is caused by the extra prepreg layer in the fabricated prototype, which was not present in Fig. 3. Corresponding to $f_0 = 14.5$ GHz, the circumference of each ring in the array is about $2.1\lambda_0$ and the antenna is about $4.8\lambda_0$ long, along the y-axis.

IV. Conclusions

A planar ME-dipole antenna array based on CRLH transmission lines has been proposed and demonstrated by full-wave and experimental results. The series elements of the CRLH transmission lines form the M-dipoles and the shunt elements form the E-dipoles. The balanced condition of CRLH transmission lines has been exploited in order to form high-gain magnetic radiators in conjunction with conventional electric radiators which are excited simultaneously using a single differential feed. The travelling-wave-type nature of the proposed structure enables the formation of directive arrays with high-gain characteristics.

By operating the antenna at the transition frequency of the antenna, uniform current can be maintained across the rings to achieve high-peak M-dipole gain. However, at frequencies different from the transition frequency, the gain drops from its peak values as a result of formation of nonuniform currents, thereby making the proposed structure narrowband in nature. In addition, due to the CRLH balancing requirements, the series and shunt elements cannot be tuned to control the E- and M-dipole gains independently. However, by controlling the size of the ring, the E- and M-dipole gains may be equalized.

The proposed ME-dipole antenna array is a dual-polarized antenna. While offering an unconventional radiation characteristic combining magnetic and electric dipole radiation, it may be customized and adapted to different requirements, such as in applications involving beam-switching or space diversity. For example, by simultaneously exciting the two differential ports of the structure with an appropriate polarity, using switches and hybrids, one may selectively excite the electric or magnetic dipole arrays only, and corresponding patterns; in the former case, one obtains a maximum at broadside, while in the latter case, one obtains a null at broadside. This reconfigurability might be applied to fixed-point systems with different target directions [4]. Similar functionality may be obtained with a single source by operating in a resonant configuration, using a short or a open circuit at the second port of the array, to selectively excite either the series or shunt resonances of the CRLH structure, which are responsible for the M- and E-dipole radiation [14], [34]. The antenna, depending on the scheme used, may thus be used as a purely magnetic loop array, or an electric-dipole array, or in a hybrid configuration where the two radiations are used in tandem in a time-domain multiplexing manner. Another application would be beam diversity for high-speed wireless communications (e.g., MIMO), where the antennas switch to different modes (single electric dipole, single magnetic dipole, or both dipoles) to pick the best channels in real time [35]. The proposed antenna thus exhibits great flexibility and versatility in its radiation characteristics, and may lead to innovative phase-array systems and applications in the future.

Acknowledgment

Authors would like to thank Z. Ma from the University of Hong Kong and Dr. K. Kan So from the City University of Hong Kong for their help in the fabrication and measurements of various prototypes. The authors would like to particularly thank the State Key Laboratory of Millimeter Waves at the City University of Hong Kong for providing the measurement facilities.

References

[1] K. M. Luk and B. Wu, "The magnetoelectric dipole, a wideband antenna for base stations in mobile communications," *Proc. IEEE*, vol. 100, no. 7, pp. 2297–2307, Jul. 2012.

[2] T. Nakanishi, T. Yoshida, A. Ishida, H. Uno, and Y. Saito, "Multiple-loop array antenna with switched beam for short-range radars," in *Proc. 64th Veh. Technol. Conf.*, Sep. 2006, pp. 1–5.

[3] J. Xiong, M. Zhao, H. Li, Z. Ying, and B. Wang, "Collocated electric and magnetic dipoles with extremely low correlation as a reference antenna for polarization diversity MIMO applications," *IEEE Antennas Wireless Propag. Lett.*, vol. 11, no. 6, pp. 423–426, Apr. 2012.

[4] S. Abielmona, H. V. Nguyen, and C. Caloz, "CRLH LWA with polarization diversity using equalized common and differential modes," presented at the IEEE AP- S Int. Antennas Propag, Chicago, IL, USA, Jul. 2012.

[5] K. Wei, Z. Zhang, Z. Feng, and M. F. Iskander, "A MNG-TL loop antenna array with horizontally polarized omnidirectional patterns," *IEEE Trans. Antennas Propag.*, vol. 60, no. 6, pp. 2702–2709, Jun. 2012.

[6] M. Callendar, "Aperiodic loop antenna arrays," in *Proc. Antennas Propag. Soc. Int. Symp.*, Dec. 1969, pp. 193–198.

[7] P. Loghmannia, M. Kamyab, M. N. Ranjbar, and R. Rezaiesarlak, "Miniaturized low-cost phased array antenna using siw slot elements," *IEEE Microw. Wireless Compon. Lett.*, pp. 1434–1437, Nov. 2012.

[8] A. Clavin, "A new antenna feed having equal E-and H-plane patterns," *IRE Trans. Antennas Propag.*, vol. AP-2, pp. 113–119, Apr. 1954.

[9] R. W. P. King and G. H. Owyang, "The slot antenna with coupled dipoles," *IRE Trans. Antennas Propag.*, vol. AP-8, pp. 136–143, Mar. 1960.

[10] P. L. Overfelt, D. R. Bowling, and D. J. White, "A colocated magnetic loop, electric dipole array antenna (preliminary results)," in *NAWCWPNS Tech Pub 8212, Naval Air Warfare Center Weapons Division*, China Lake, CA, USA, Sep. 1994.
[11] M. Li and K.-M. Luk, "A differential-fed magneto-electric dipole antenna for UWB applications," *IEEE Trans. Antennas Propag.*, vol. 61, no. 1, pp. 92–99, Jan. 2013.
[12] K. M. Luk and H. Wong, "A new wideband unidirectional antenna element," *Int. J. Microw. Opt. Technol.*, vol. 1, pp. 35–44, Apr. 2006.
[13] C. Caloz, T. Itoh, and A. Rennings, "CRLH metamaterial leaky-wave and resonant antennas," *IEEE Antennas Propag. Mag.*, vol. 50, no. 5, pp. 25–39, Oct. 2008.
[14] C. Caloz and T. Itoh, *Electromagnetic Metamaterials, Transmission Line Theory and Microwave Applications*. Hoboken, NJ, USA: Wiley/IEEE, 2005.
[15] M. R. M. Hashemi and T. Itoh, "Dual-mode leaky-wave excitation in symmetric composite right/left-handed structure with center vias," in *Proc. IEEE MTT-S Int. Microw. Symp.*, Anaheim, CA, USA, May 2010, vol. 100, pp. 9–12.
[16] M. R. M. Hashemi and T. Itoh, "Coupled composite right/left-handed leaky-wave transmission-lines based on common/differential-mode analysis," *IEEE Trans. Microw. Theory Tech.*, vol. 58, no. 12, pp. 3645–3656, Dec. 2010.
[17] C. A. Balanis, *Advanced Engineering Electromagnetics*. New York, USA: Wiley, 1989.
[18] G. Eleftheriades and K. Balmain, *Negative-Refraction Metamaterials: Fundamental Principles and Applications*. Hoboken, NJ, USA: Wiley/IEEE, 2005.
[19] F. Capolino, *Metamaterials Handbook: Applications of Metamaterials*. Boca Raton, FL, USA: CRC, 2009.
[20] S. Paulotto, P. Baccarelli, F. Frezza, and D. R. Jackson, "Full-wave modal dispersion analysis and broadside optimization for a class of microstrip crlh leaky-wave antennas," *IEEE Trans. Microw. Theory Tech.*, vol. 56, no. 12, pp. 2826–2837, Dec. 2008.
[21] C. Caloz, "Perspectives on EM metamaterials," *Mater. Today*, vol. 12, no. 3, pp. 12–30, Mar. 2009.
[22] M. A. Y. Abdalla, K. Phang, and G. V. Eleftheriades, "A planar electronically steerable patch array using tunable pri/nri phase shifters," *IEEE Trans. Microw. Theory Tech.*, vol. 57, no. 3, pp. 531–541, Mar. 2009.
[23] Y.-K. Jung and B. Lee, "Beam scannable patch array antenna employing tunable metamaterial phase shifter," in *Proc. IEEE Antennas Propag. Soc. Int. Symp.*, Jul. 2012, vol. 57, no. 3, pp. 1–2.
[24] A. Locatelli, A. Capobianco, S. Boscolo, D. Modotto, M. Midrio, and C. D. Angelis, "Low-profile CRLH omnidirectional loop antenna for mobile wireless communications," *Proc. 42nd Eur. Microw. Conf.*, pp. 401–403, Oct. 2012.
[25] J.-G. Lee and J.-H. Lee, "Zeroth order resonance loop antenna," *IEEE Trans. Antennas Propag.*, vol. 55, no. 3, pp. 994–997, Mar. 2007.
[26] C. Caloz, D. R. Jackson, and T. Itoh, *Frontiers in Antennas*, F. Gross, Ed. New York, USA: McGraw-Hill, 2010.
[27] D. R. Jackson, C. Caloz, and T. Itoh, "Leaky-wave antennas," *Proc. IEEE*, vol. 100, no. 7, pp. 2194–2206, Jul. 2012.
[28] S. Otto, A. Rennings, K. Solbach, and C. Caloz, "Transmission line modeling and asymptotic formulas for periodic leaky-wave antennas scanning through broadside," *IEEE Trans. Antennas Propag.*, vol. 59, no. 10, pp. 3695–3709, Oct. 2010.
[29] N. Yang, C. Caloz, and K. Wu, "Greater than the sum of its parts," *Microw. Mag.*, vol. 11, no. 4, pp. 69–82, Jun. 2010.
[30] J. Karki, "Fully differential amplifiers," Texas Instruments, Dallas, TX, USA, TI Appl. Rep. SLOA054D, Jan. 2002.
[31] F. P. Casares-Miranda, C. Camacho-Pe-alosa, and C. Caloz, "High-gain active composite right/left-handed leaky-wave antenna," *IEEE Trans. Antennas Propag.*, vol. 54, no. 8, pp. 2292–2300, Aug. 2006.
[32] K. Mori and T. Itoh, "Distributed amplifier with CRLH-transmission line leaky wave antenna," in *Proc. 38th Eur. Microw. Conf.*, Oct. 2008, pp. 686–689.
[33] C. Caloz and T. Itoh, "Array factor approach of leaky-wave antennas and application to 1D/2D composite right/left-handed (CRLH) structures," *IEEE Microw. Wireless Compon. Lett.*, vol. 14, no. 6, pp. 274–276, Jun. 2004.
[34] M. R. M. Hashemi and T. Itoh, "Evolution of composite right/left-handed leaky-wave antennas," *Proc. IEEE*, vol. 99, no. 10, pp. 1746–1754, Oct. 2011.
[35] J.-F. Frigon, C. Caloz, and Y. Y. Zhao, "Dynamic radiation pattern diversity (DRPD) MIMO using CRLH leaky-wave antennas," presented at the IEEE Radio Wireless Symp., Orlando, FL, USA, Jan. 2008.

Shulabh Gupta (M'11) was born on December 14, 1982, in India. He received the B.Tech. degree in electronic engineering from the Indian School of Mines, Dhanbad, India, in 2004, the M.S. degree in telecommunications from Institut National de la Recherche Scientifique Énergie Matériaux Télécommunications Research Center (INRS-EMT), Université du Quebec, Montréal, QC, Canada, in 2006, and the Ph.D. degree in electrical engineering from the École Polytechnique of Montréal, Montréal, in 2012.

His M.S. thesis research focused on optical signal processing related to the propagation of light in linear and nonlinear optical fibers and fiber Bragg gratings. His Ph.D. research concerned the analog signal-processing techniques using dispersion-engineered structures. From 2009 to 2010, he was a Visiting Research Fellow with the Tokyo Institute of Technology, Tokyo, Japan, where he was involved in the application of high-impedance surfaces for oversized slotted waveguide antennas. He was a Postdoctoral Fellow at the University of Colorado, Boulder, after completing the Ph.D. degree in 2012, where he was working on the design and characterization of high-power ultrawideband antennas. He later joined the University of Hong Kong, 2012–2014 as a Postdoctoral Fellow where his research focused on multifunctional travelling-wave leaky-wave antennas for radio-frequency identification and imaging applications.

Dr. Gupta was a recipient of the Young Scientist Award of EMTS Ottawa 2007, URSI-GA, Chicago 2008, and ISAP Jeju 2011. His thesis won the best doctoral dissertation award in 2012 at the École Polytechnique of Montréal in 2012, Prix dexcellence de lAssociation des doyens des études supérieures au Québec (ADÉSAQ) Édition 2013 in Quebec, and the Academic Gold Medal of the Governor General of Canada.

Li Jun Jiang (SM'13) received the B.S. degree in electrical engineering from the Beijing University of Aeronautics and Astronautics, Beijing, China, in 1993, the M.S. degree in electrical engineering from the Tsinghua University, Beijing, in 1996, and the Ph.D. degree in electrical and computer engineering from the University of Illinois at Urbana-Champaign, IL, USA, in 2004.

From 1996 to 1999, he was an Application Engineer with the Hewlett-Packard Company, Beijing, China. Since 2004, he has been the Postdoctoral Researcher, the Research Staff Member, and the Senior Engineer at IBM T. J. Watson Research Center, New York, USA. Since 2009, he has been an Associate Professor with the Department of Electrical and Electronic Engineering, University of Hong Kong, Hong Kong, China. His research interests focus on electromagnetics, computational electromagnetics, integrated-circuit (IC) signal/power integrity, IC electromagnetic compatibility/electromagnetic interference, antennas, and multiphysics modeling.

In 1998 he received the HP STAR Award. In 2003, he received the IEEE MTT Graduate Fellowship Award, and in 2004, the Y. T. Lo Outstanding Research Award. In 2008, he received the IBM Research Technical Achievement Award. He is the Associate Editor of IEEE TRANSACTIONS ON ANTENNAS AND PROPAGATION, the Editor of *Progress in Electromagnetics Research*, the Associate Guest Editor of the PROCEEDINGS IEEE SPECIAL ISSUE in 2011 and 2012, an IEEE AP-S Member, an IEEE MTT-S member, an ACES member, and a member of the Chinese Computational Electromagnetics Society. He was the Semiconductor Research Cooperation (SRC) Industrial Liaison for several academic projects. He has been the Technical Programme Committee (TPC) member of IEEE Electrical Design for Advanced Packaging and Systems (EDAPS) since 2010, the TPC member of the 2013 IEEE International Conference on Microwave Technology & Computational Electromagnetics (ICMTCE), the scientific committee member of the 2010 Workshop on Simulation and Modeling of Emerging Electronics (SMEE), the special session organizers of IEEE EDAPS, the International Review of Progress in Applied Computational Electromagnetics (ACES), Asia-Pacific Radio Science Conference (AP-RASC), the co-organizer of HKU Computational Science and Engineering Workshops in 2010–2012, the TC-9 and TC-10 member of IEEE EMC-S since 2011, the TPC Chair of the 7th International Conference on Nanophotonics (ICNP), the TPC member of the 3rd Conference on Advances in Optoelectronics and Micro/Nano Optics (AOM), the Co-Chair of International Workshop on Pulsed Electromagnetic Field 2013, the Chair of 14th IEEE Hong Kong AP/MTT Postgraduate Conference, and session chairs of many international conferences. He also serves as the reviewer of IEEE

TRANSACTIONS on several topics, and other primary electromagnetics and microwave-related journals.

Christophe Caloz (F'10) received the Ph.D. degree in sciences from École Polytechnique Fédérale de Lausanne (EPFL), Lausanne, Switzerland, in 2000.

From 2001 to 2004, he was a Postdoctoral Research Engineer with the Microwave Electronics Laboratory of University of California at Los Angeles (UCLA). In 2004, he joined École Polytechnique of Montréal, Montréal, QC, Canada, where he is a Full Professor, a member of the Poly-Grames Microwave Research Center, and the holder of a Canada Research Chair (CRC). He has authored and coauthored more than 500 technical conference, letter, and journal papers, 12 books and book chapters, and he holds several patents. His works have generated about 10 000 citations. In 2009, he co-founded the company ScisWave, Montréal, which develops CRLH smart-antenna solutions for WiFi. His research interests include all fields of theoretical, computational, and technological electromagnetics, with a strong emphasis on emerging and multidisciplinary topics, including particularly metamaterials, nanoelectromagnetics, exotic antenna systems, and real-time radio.

Dr. Caloz is a member of the Microwave Theory and Techniques Society (MTT-S) technical committees MTT-15 (Microwave Field Theory) and MTT-25 (RF Nanotechnology), a Speaker of the MTT-15 Speaker Bureau, the Chair of the Commission D (Electronics and Photonics) of the Canadian Union de Radio Science Internationale (URSI), and an MTT-S representative at the IEEE Nanotechnology Council (NTC). He received several awards, including the UCLA Chancellors Award for Postdoctoral Research in 2004, the MTT-S Outstanding Young Engineer Award in 2007, the E. W. R. Steacie Memorial Fellowship in 2013, the Prix Urgel-Archambault in 2013, and many best paper awards with his students at international conferences. He has been an IEEE Distinguished Lecturer for the Antennas and Propagation Society (AP-S) since 2014.